Mathematical modeling of calcium-mediated exosomal dynamics in neural cells

Shaheen, H., Singh, S. and Melnik, R.

Advances in Nonlinear Dynamics, Vol. 3, 83-92, 2022.

Proceedings of the Second International Nonlinear Dynamics Conference (NODYCON 2021), Eds.: W. Lacarbonara, B. Balachandran, M. J. Leamy, J. Ma, J. A. T. Machado, G. Stepan.
Springer, 2022.

DOI: 10.1007/978-3-030-81170-9_8

Mathematical modeling of calcium-mediated exosomal dynamics in neural cells

Hina Shaheen[1*], Sundeep Singh[1], and Roderick Melnik[1,2]

[1] MS2Discovery Interdisciplinary Research Institute, Wilfrid Laurier University, 75 University Avenue West, Waterloo, Ontario, N2L 3C5, Canada
[2] BCAM - Basque Center for Applied Mathematics, Alameda de Mazarredo 14, E-48009 Bilbao, Spain
shah8322@mylaurier.ca

Abstract. An exosome-mediated drug delivery system has received significant attention for the treatment of neurological disorders, such as Parkinson's disease. In this contribution, we report a more realistic mathematical model for capturing the calcium (Ca^{2+})-mediated exosomal release in the neural stem cells. The modified Hodgkin-Huxley neuronal model has been used to characterize a depolarized neuron's electrical activity via membrane potential for action potential initiation and propagation. The intracellular Ca^{2+} dynamics have been modeled by coupling the neuronal electrical activity and Ca^{2+}-mediated exocytosis, taking into account the high-voltage (L-type) and low-voltage (T-type) activated Ca^{2+} channels, plasma membrane, bulk cytosol and endoplasmic reticulum. The novelty of the present paper includes also a comparative analysis, carried out for the first time, to quantify the effect of temperature on the Ca^{2+}-mediated exosomal release in the neurons. The study revealed that the variation in temperature results in an increase of the sodium/potassium currents that leads to the spatio-temporal variations of calcium concentrations. It is expected that the proposed model would provide a more comprehensive understanding of the key mechanisms underlying the dynamics of various brain diseases.

Keywords: Brain, calcium channels, exosomes, molecular communication, temperature effects, neural stem cells

1 Introduction

The intracellular calcium (Ca^{2+}) concentration plays a critical role in synaptic transmission and neuronal excitability, along with other neural dysfunction associated with chronic brain disorders. Moreover, intracellular Ca^{2+} concentration influences multiple cellular functions, including enzyme and release activities and the signaling of numerous plasma membranes [1]. Chronic exposure to high concentrations of the Ca^{2+} can cause neurotoxicity, which is a neurological syndrome consisting of movement abnormalities that share many Parkinsonian features. Intracellular Ca^{2+} is an important neuronal signal transduction mediator, taking part in assorted biochemical reactions that evoke changes in synaptic

adequacy, metabolic rate, and gene transcription. Although measurement of intracellular Ca^{2+} in living neurons through fluorescent Ca^{2+} markers has not reliably demonstrated a link between cytosolic Ca^{2+} and the occurrence of neuronal death, excessive cytosolic calcium has been implicated as a cause of acute neuronal injury [2].

Neurodegenerative disorders represent a heterogeneous group of diseases characterized by progressive structural and functional aggregation of misfolded proteins. It has been recently shown that these aggregated proteins may be exchanged from one cell to another through extracellular nanovesicles called exosomes [3]. Exosomes are mostly found in all kinds of biological fluids and are basically 40-100 nm sized extracellular vesicles comprising of natural lipid bilayers [4]. It has been revealed that the content of the exosomes inferred from the central nervous system is altered during disease, making them an appealing target for biomarker development of multiple neurodegenerative disorders, viz., Alzheimer, Parkinson, Huntington and Creutzfeldt-Jacob [5]. Exosome release from neurons, astrocytes and neural cell lines triggered by depolarization-induced increased intracellular Ca^{2+} leads to the interesting possibility that activity-dependent regulation of exosome release could provide a mechanism to control neural dysfunction and temporal features of exosome in the brain [12]. Owing to their biological tolerability, exosomes provide exciting opportunities for delivering chemical chemical components to a target cell, thereby assisting in developing novel diagnostic and therapeutic approaches [6, 11].

A recent study found that when differentiated neurons and astrocytes are depolarized, specific types of Ca^{2+} channels in differentiated neurons and astrocytes are activated, resulting in increased intracellular Ca^{2+} concentration levels, which interfere with the mobilisation of multivesicular bodies and exosomal release [8]. There's the exploratory prove that: (a) in neurons, glutamatergic movement is improved by depolarization and an increment within the intracellular Ca^{2+} which assists with upgraded exosomal secretion and (b) intracellular Ca^{2+} levels regulate vesicular secretion and release in astrocytes [8]. To provide a platform towards Ca^{2+}-mediated exosomal dynamics, we propose a more realistic mathematical model for capturing the Ca^{2+}-mediated exosomal release in the neural stem cells. Here we will focus on the novel aspects of regulated therapeutic exosomal release by introducing mathematical models as a framework for optimizing neural models that combine depolarization, intracellular Ca^{2+} concentrations and vesicular exocytosis. The electrical activity of a depolarized neuron via membrane potential for action potential initiation and propagation is investigated using the modified Hodgkin-Huxley neuronal model. The intracellular Ca^{2+} dynamics have been modelled by coupling the neuronal electrical activity and Ca^{2+}-mediated exocytosis, taking into account the high-voltage (L-type) and low-voltage (T-type) activated Ca^{2+} channels, plasma membrane, bulk cytosol and endoplasmic reticulum. Furthermore, the effects of temperature on the modulated Ca^{2+}-mediated exosomal release in the neurons has also been studied that could assist in developing more accurate methods for regulating neural activity [9].

2 Mathematical model of Ca^{2+}-mediated exosomal dynamics

The present study aims at modeling the Ca^{2+}-mediated exosomal dynamics in brain differentiated into neurons considering two different approaches: (i) a simplified neuronal model consisting of intracellular Ca^{2+} dynamics with a special focus on microdomain $Ca2+$ concentrations and (ii) a more realistic neuronal model accounting for temperature effects on the intracellular Ca^{2+} dynamics with gated conductances.

A better understanding of the Ca^{2+} ions dynamics in the central nervous system could serve as a testing bed for decoding synaptic exocytosis mechanism, e.g., synaptic vesicle docking, diffusion, and neurotransmitter release. In this section, we develop a comprehensive model of Ca^{2+} dynamics and exocytosis in neurons downstream of electrical activity. Exosomal release mediated by Ca^{2+} is limited to active zones, which contain voltage-gated Ca^{2+} channels that govern Ca^{2+} from the extracellular domain, mediate, and regulate exocytosis, and lead to exosomal release in the brain. The proposed model is used to analyze the coupling between electrical activity and Ca^{2+}-mediated exosomal release. We first analyze the intracellular Ca^{2+} dynamics along with the microdomain Ca^{2+} concentrations surrounding high-voltage active L-type ($[Ca]_L$) and low-voltage T-type Ca^{2+} channels (when they open and close), connected beneath the plasma membrane ($[Ca]_m$), within the endoplasmic reticulum ($[Ca]_{ER}$) and in the bulk cytosol ($[Ca]_c$). The model is developed combining Watts-Sherman and Montefusco-Pedersen models for Ca^{2+}-mediated exosomal release and regulated exocytosis as [8]:

$$\frac{d[Ca]_{L|opened}}{dt} = -f\bigg(\alpha\frac{i_{Ca_L}}{V_{ud}} - B_{ud}([Ca]_L - [Ca]_m)\bigg), \tag{1}$$

$$\frac{d[Ca]_m}{dt} = \frac{f}{V_m}\bigg(- \alpha i_{Ca_T} + N_L V_{ud} B_{ud} m_{Ca_L}^2 h_{Ca_L}([Ca]_L - [Ca]_m) - V_c k_{PMCA}[Ca]_m - V_c B_M([Ca]_m - [Ca]_c)\bigg), \tag{2}$$

$$\frac{d[Ca]_c}{dt} = f(B_m([Ca]_m - [Ca]_c) + p_{leak}([Ca]_{ER} - [Ca]_c) - k_{SERCA}[Ca]_c), \tag{3}$$

$$\frac{d[Ca]_{ER}}{dt} = \frac{fV_c}{V_{ER}}(p_{leak}([Ca]_{ER} - [Ca]_c) - k_{SERCA}[Ca]_c), \tag{4}$$

where $i_{Ca_L} = (g_{Ca_L}(v_m - V_{Ca}))/N_L$ is the Ca^{2+} current entering the L-Type Ca^{2+} channel, $i_{Ca_T} = g_{Ca_T} m_{Ca_T}^3 h_{Ca_T}(v_m - V_{Ca})$ is the Ca^{2+} current entering through T-type Ca^{2+} channel, g_{Ca_L} is the membrane conductance of the L-type Ca^{2+} channel, g_{Ca_T} is the membrane conductance of T-type Ca^{2+} channel, $m_{Ca_L}^2 h_{Ca_L}$ and $m_{Ca_T}^3 h_{Ca_T}$ represent the opening probability for the L-type and T-type Ca^{2+} channels, respectively, and N_L is the number of L-type Ca^{2+}

channels [8]. α is the constant that converts current to flux, f is the ratio of free-to-total Ca^{2+}, B_m is the flux from sub-membrane compartment to bulk cytosol, $B_{\mu d}$ is the constant flux from microdomains to sub-membrane, k_{PMCA} is the rate of Ca^{2+} adenosine triphosphatase (ATPase) through the plasma membrane, p_{leak} is the rate of the leak current from the ER to the cytosol, and k_{SERCA} is the rate of Sarco/endoplasmic Ca^{2+} ATPase pump-dependent sequestration of Ca^{2+} into the ER, V_d, V_m, V_c and V_{ER} are the volumes of single microdomain, sub-membrane compartment, bulk cytosol, and ER, respectively [8]. The gating variables are defined as:

$$\frac{dm_x}{dt} = \frac{m_{x,\infty}(v_m) - mx}{\tau_{mx(v_m)}};\ \frac{dh_x}{dt} = \frac{h_{x,\infty}(v_m) - hx}{\tau_{hx(v_m)}}, \tag{5}$$

where $x \in (Ca_L, Ca_T, Na, K)$ and

$$\begin{cases} m_{K/Na,\infty} = \frac{\alpha_{m_{K/Na}}}{\alpha_{m_{K/Na}}+\beta_{m_{K/Na}}};\ h_{Na,\infty} = \frac{\alpha_{h_{Na}}}{\alpha_{h_{Na}}+\beta_{h_{Na}}}, \\ \tau_{h_{Na}} = \frac{1}{\alpha_{h_{Na}}+\beta_{h_{Na}}};\ \tau_{m_{K/Na}} = \frac{1}{\alpha_{m_{K/Na}}+\beta_{m_{K/Na}}}, \\ \alpha_{m_{Na}} = \frac{(0.1(v_m+40))}{(1-exp(-(v_m+40)/10))};\ \beta_{m_{Na}} = \frac{(4exp(-(v_m+65))}{18}, \\ \alpha_{m_K} = \frac{(0.01(v_m+55))}{1-exp(-(v_m+55)/10)};\ \beta_{m_K} = \frac{0.125exp(-(v_m+65))}{80}, \\ \alpha_{h_{Na}} = \frac{(0.07exp(-(v_m+65)))}{20};\ \beta_{h_{Na}} = \frac{1}{1+exp(-(v_m+35)/10)}. \end{cases} \tag{6}$$

Time constants and the gating variables in the steady state for $x \in (T, L)$ are defined as:

$$\begin{cases} m_{Ca_x,\infty} = \frac{1}{1+exp(\frac{-(v_m-V_{m_{Ca_x}})}{S_{m_{Ca_x}}})};\ h_{Ca_x,\infty} = \frac{1}{1+exp(\frac{-(v_m-V_{h_{Ca_x}})}{S_{h_{Ca_x}}})}, \\ \tau_{m_{Ca_x}} = \frac{\tau_{m_{V_{Ca_x}}}}{exp(\frac{-(v_m-V_{\tau_{m_{Ca_x}}})}{S_{\tau_{m_{Ca_x}}}})+exp(\frac{(v_m-V_{\tau_{m_{Ca_x}}})}{S_{\tau_{m_{Ca_x}}}})} + \tau_{m0_{V_{Ca_x}}}, \\ \tau_{h_{Ca_x}} = \frac{\tau_{h_{V_{Ca_x}}}}{exp(\frac{-(v_m-V_{\tau_{h_{Ca_x}}})}{S_{\tau_{h_{Ca_x}}}})+exp(\frac{(v_m-V_{\tau_{h_{Ca_x}}})}{S_{\tau_{h_{Ca_x}}}})} + \tau_{h0_{V_{Ca_x}}}. \end{cases} \tag{7}$$

The relative exosomal release rate in neurons depending on L-type Ca^{2+} microdomain concentrations and plasma membrane Ca^{2+} concentrations can be represented, respectively, as follows [8]:

$$R_{Ca_L} = m^2_{Ca_L} h_{Ca_L} F_H([Ca]_{L|opened}, K_L, n_L) + (1 - m^2_{Ca_L} h_{Ca_L}) F_H([Ca]_{L|closed}, K_L, n_L), \tag{8}$$

$$R_{Ca_m} = F_H([Ca]_m, K_m, n_m), \tag{9}$$

where $F_H(x, K, n) = \phi \frac{x^n}{x^n+K^n}$ is the Hill function, $[Ca]_{L|closed} = [Ca]_m$ and ϕ is a fusion constant given in s^{-1} [8]. Experimental evidences have revealed that Ca^{2+}-mediated exocytosis by neurons is regulated by intracellular Ca^{2+} where Ca^{2+} threshold of exocytosis depends on the pattern of electrical activity [8]. The electrical activity triggered by the neuron depolarization includes the activation of voltage-gated Ca^{2+} channels upon cell depolarization, due to increased

intracellular Ca^{2+} concentration levels, which interfere with the mobilisation of multivesicular bodies, resulting in exosome release and exocytosis. As mentioned, we adopt the modified Hodgkin-Huxley neuron model for describing the neural signals of a depolarized neuron via membrane potential (v_m) that depends on voltage-gated potassium (K^+) channel, voltage-gated sodium (Na^+) channel, leak current and induced control signal/current (i_{ind}) as [8]:

$$\frac{dv_m}{dt} = \frac{-1}{C_m}\Big[g_K(v_m - V_K) + g_{Na}(v_m - V_{Na}) + g_L(v_m - V_L) - i_{ind}\Big], \quad (10)$$

where C_m is the membrane capacitance, V_K, V_{Na}, V_{Ca} and V_L are Nernst potentials for K^+, Ca^{2+} and Na^+ ions and other ions clubbed as a leak channel, respectively, and g_K, V_{Na} and g_L are the corresponding membrane conductances. Voltage gated conductances ($g_K = \bar{g_K} m_K^4$ and $g_{Na} = \bar{g_{Na}} m_{Na}^3 h_{Na}$) change with time during the action potential initiation and dissemination. Moreover, m_K^4 and $m_{Na}^3 h_{Na}$ represent the opening probability for K^+ and Na^+ channel. The gating variables m_K, m_{Na} and h_{Na} are defined in Eq. 7. Furthermore, we will construct a more realistic neuronal model where the main characteristics account for temperature effects on Ca^{2+}-mediated exosomal release in the neurons. Potassium currents exceed sodium currents at higher temperatures, resulting in action potential failure. Thermal inhibition may, however, be explained by other temperature-dependent alterations [9]. Therefore, understanding the effects of temperature on Ca^{2+}-mediated exosomal release may be extremely useful in developing more accurate methods of regulating neural activity in the brain. We will use the modified Hodgkin-Huxley model to capture the response of Ca^{2+}-mediated exosomal release in the neurons by varying the peak sodium and potassium conductances with temperature. It has been shown that the resting potential varies with the temperature [9]. In the simplified neuronal model, the peak sodium and potassium conductances $\bar{g_{Na}}$ and $\bar{g_K}$ were assumed to be constant and independent of temperature, but these values vary with temperature for a more realistic neuronal model i.e ($g_K = g_{Kmax}(T) m_K^4$ and $g_{Na} = g_{Namax}(T) m_{Na}^3 h_{Na}$) , where $g_{Kmax}(T) = 1.60e^{-}(\frac{T-27.88}{12.85})^2$, $g_{Namax}(T) = 0.42e^{-}(\frac{T-31.83}{31.62})^2$ [8]. Thus, while modeling the temperature effects, only the membrane potential, given in Eq. 10, will be modified and the peak conductances values will be computed from the temperature-dependent gating variables defined as:

$$\begin{cases} \frac{dm_{K/Na}}{dt} = \phi_{m_{K/Na}}(T)(\alpha_{m_{K/Na}}(1 - m_{K/Na}) - \beta_{m_{K/Na}} m_{K/Na}), \\ \frac{dh_{Na}}{dt} = \phi_{h_{Na}}(T)(\alpha_{h_{Na}}(1 - h_{Na}) - \beta_{h_{Na}} h_{Na}), \end{cases} \quad (11)$$

where

$$\begin{cases} \phi_{m_K}(T) = 3^{\frac{10-6.3}{10}} 3^{\frac{15-10}{10}} 2.8^{\frac{20-15}{10}} 2.7^{\frac{T-20}{10}}, \\ \phi_{m_{Na}}(T) = 3^{\frac{10-6.3}{10}} 2.9^{\frac{15-10}{10}} 3^{\frac{20-15}{10}} 3^{\frac{T-20}{10}}, \\ \phi_{h_{Na}}(T) = 3^{\frac{10-6.3}{10}} 2.8^{\frac{15-10}{10}} 2.4^{\frac{20-15}{10}} 2.3^{\frac{T-20}{10}}, \end{cases} \quad (12)$$

are adopted from [9] for the considered temperature of 25 ^{o}C.

Table 1. Parameter set for calcium-mediated exosomal dynamics.

Parameter	Value	Parameter	Value	Parameter	Value
V_K	$-70(mV)$	V_L	$-54.4(mV)$	$V_{h_{Ca_T}}$	$-52(mV)$
$V_{\tau_{h_{Ca_T}}}$	$-50(mV)$	$V_{\tau_{m_{Ca_T}}}$	$-50(mV)$	$V_{\tau_{h_{Ca_L}}}$	$0(mV)$
$V_{m_{Ca_T}}$	$-49(mV)$	$V_{h_{Ca_L}}$	$-33(mV)$	$V_{m_{Ca_L}}$	$-30(mV)$
$V_{\tau_{m_{Ca_L}}}$	-23(mV)	$S_{h_{Ca_L}}$	$-5(mV)$	$S_{h_{Ca_T}}$	$-5(mV)$
$\tau_{m0_{V_{Ca_T}}}$	$0(ms)$	V_{ud}	$2.62 \times 10^{-19}(L)$	α	$5 \times 10^{-15}(\mu molpm/As)$
V_m	$5 \times 10^{-14}(L)$	V_c	$5.7 \times 10^{-13}(L)$	p_{leak}	$3 \times 10^{-4}(ms^{-1})$
f	0.01	$\tau_{m0_{V_{Ca_L}}}$	$0.05(ms)$	k_{SERCA}	$0.100(ms^{-1})$
B_m	$0.128(ms^{-1})$	g_L	$0.3(mS/cm^3)$	k_{PMCA}	$0.300(ms^{-1})$
g_{Ca_T}	$0.4(nS)$	g_{Ca_L}	$0.7(nS)$	C_m	$1(uF/cm^2)$
$\tau_{m_{V_{Ca_L}}}$	$1(ms)$	K_m	$2(uM)$	n_L	4
n_m	4	$S_{m_{Ca_T}}$	$4(mV)$	$\tau_{h0_{V_{Ca_T}}}$	$5(ms)$
$S_{m_{Ca_L}}$	$10(mV)$	T	10^oC	$S_{\tau_{m_{Ca_T}}}$	$12(mV)$
$\tau_{m_{V_{Ca_T}}}$	$15(ms)$	$S_{\tau_{h_{Ca_T}}}$	$15(mV)$	$S_{\tau_{m_{Ca_L}}}$	$20(mV)$
$S_{\tau_{h_{Ca_L}}}$	$20(mV)$	$\tau_{h_{V_{Ca_T}}}$	$20(ms)$	$\frac{V_c}{V_{ER}}$	31
$\bar{g_K}$	$36(mS/cm^3)$	V_{Na}	$50(mV)$	K_L	$50(\mu M)$
$\tau_{h0_{V_{Ca_L}}}$	$51(ms)$	$\tau_{h_{V_{Ca_L}}}$	$60(ms)$	V_{Ca}	$65(mV)$
$\bar{g_{Na}}$	$120(mS/cm^3)$	N_L	200	B_{ud}	$264(ms^{-1})$

3 Results and Discussion

In this paper, a numerical study has been performed for quantifying the effects of a control signal, membrane potential, gated conductances and temperature on Ca^{2+}-mediated exosomal dynamics in the neurons. Notably, Ca^{2+} mediated exocytosis has been quantified on the membrane potential with particular attention given to microdomain Ca^{2+} concentrations that surrounds the high-voltage L-type and low-voltage T-type Ca^{2+} channels that links to the description of Ca^{2+} within the bulk cytosol and the endoplasmic reticulum under the plasma membrane using the simplified neuronal model. Whereas the effects of temperature on the Ca^{2+}-mediated exosomal dynamics have been investigated utilizing the more realistic neuronal model. The numerical results presented in this section have been obtained using the parameter values collected from [8] and [9], as presented in Table 1. A finite element method implemented via [10] has been used to solve the set of coupled ordinary differential equations of the simplified and more realistic neuronal model.

Motivated by [8], an external stimulus has been applied to excite the neurons by applying the current pulses ranging from amplitudes of 5-20 $\mu A/cm^2$ for a duration of 500 ms, as depicted in Fig. 1a. The effects of the induced pulse of 20 $\mu A/cm^2$ on the membrane potential with temperature ($T = 25\ ^oC$) and without the temperature effects have been presented in Fig. 1b. As evident from this figure, the rate of generated sequences of the action potentials is proportional to

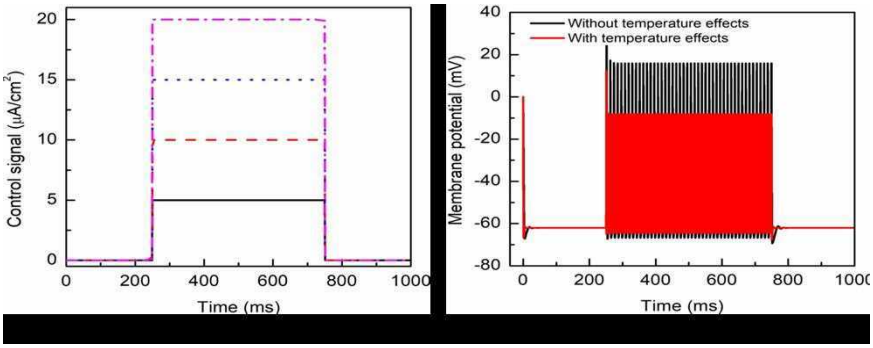

Fig. 1. (Color online) (a) Induced control signals/currents and (b) the effect of temperature on the responses/spiking sequence in the depolarized neurons for $i_{ind} = 20\mu A/cm^2$.

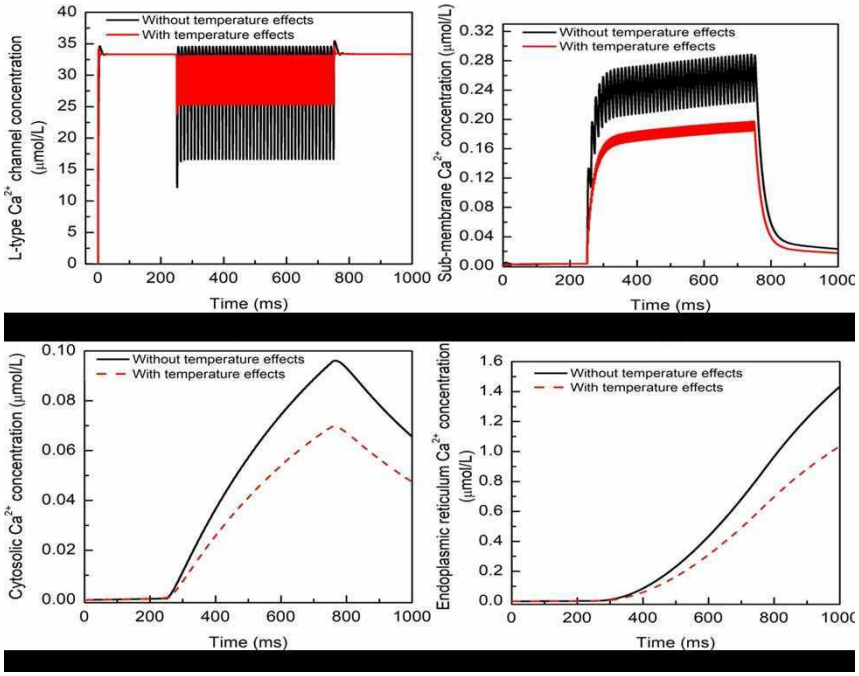

Fig. 2. (Color online) Microdomain calcium concentrations: (a) $[Ca]_L$, (b) $[Ca]_m$, (c) $[Ca]_c$ and (d) $[Ca]_{ER}$ with and without temperature effects corresponding to control signal of $i_{ind} = 20\mu A/cm^2$.

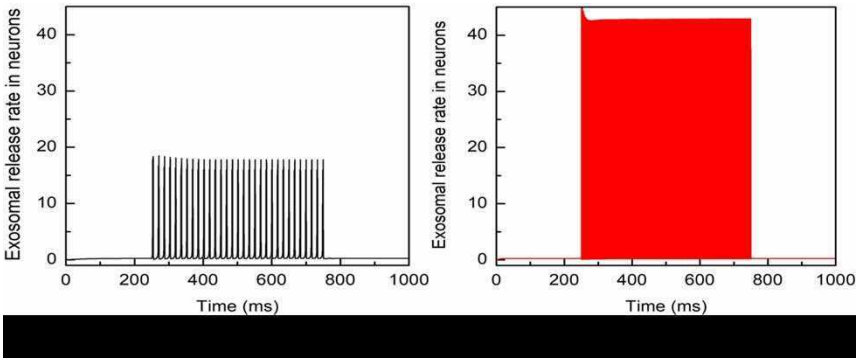

Fig. 3. (Color online) The rate of released exosomes in neurons: (a) without temperature and (b) with temperature corresponding to control signals of $i_{ind} = 20\mu A/cm^2$.

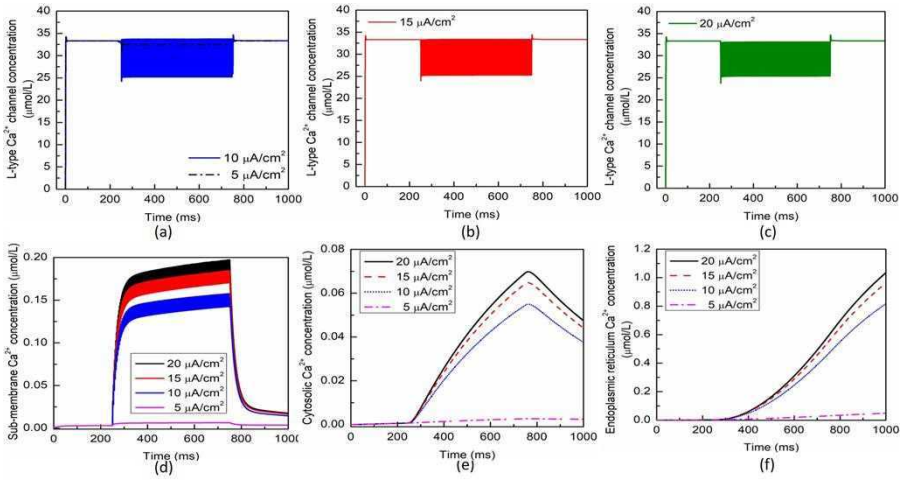

Fig. 4. (Color online) Microdomain calcium concentrations for: (a,b,c) $[Ca]_L$, (d) $[Ca]_m$, (e) $[Ca]_c$ and (f) $[Ca]_{ER}$ corresponding to control signal shown in Fig 1(a) ranging from i_{ind} = 5-20 $\mu A/cm^2$ incorporating temperature effects.

both the magnitude and duration of the external stimuli. Not only this, but the spiking sequences are also significantly reduced when the temperature effects are incorporated within the numerical model. Importantly, the voltage-gated calcium channels in the membrane are regulated by these spiking sequences [8].

The effects of the temperature on the microdomain calcium concentrations have been presented in Fig. 2. As seen from the analysis of this figure, the intracellular Ca^{2+} concentrations in the closed and open channels of L-type, plasma membrane, bulk cytosol and endoplasmic reticulum are significantly overestimated if the effect of temperature is neglected. Moreover, the exosomal release rate in neurons directly linked with the Ca^{2+} concentrations in different compartments has been presented in Fig. 3. Again, there prevail significant deviations among the two considered cases. The exosomal release rate is relatively higher when temperature effects are incorporated within the model. This can be attributed to the fact that an increase in temperature values will lead to corresponding increase in the net hyperpolarizing current. Although due to the increased speed of sodium/potassium ions gated conductances, the sodium inward current became shorter and the potassium outward current became stronger and wider. As the membrane was depolarized by the action potential, the net current became steadily outward (hyperpolarizing) with increasing temperature. Thus, the exosomal release rate of the targeted neuron is significantly affected by the changes in temperature. Further, the effect of the control signal presented in Fig. 1a on the microdomain calcium concentrations has been depicted in Fig. 4. As evident, the increase in the amplitude of the control signal stimuli from 5 to 20 $\mu A/cm^2$ results in a corresponding increase in the concentration of $[Ca]_{ER}$, $[Ca]_m]$, $[Ca]_c$ concentrations, while the effect on the $[Ca]_L$ concentration is quite negligible.

4 Conclusions

In this paper, we proposed a new numerical model for accurately quantifying the Ca^{2+}-mediated exosomal release influenced by the externally applied stimulus to the neurons accounting for temperature effects, a feature that lends potentially more realistic predictions. Our predictions suggest that cell depolarization in neurons is directly related to the exosomal release which is further proportional to the applied stimulation. The novelty of the present research is in the development of Ca^{2+}-mediated exosomal dynamics model of neurons accounting for the temperature effects. Further, it has been observed that calcium concentrations in the respective compartments and thus the overall Ca^{2+}-mediated exosomal dynamics are significantly affected by the changes in temperature. The developed neuronal model and the results presented in this study provides an important initial step not only for our better understanding of the exosomal dynamics but also paves the way for the generation of new models for optimizing and designing of exosomes-based drug delivery systems for the treatment of brain pathologies. Future studies will be focused on the inclusion of other calcium compartments,

as well as on the development of a new stochastic model based on the ideas highlighted here.

Acknowledgement

Authors are grateful to the NSERC and the CRC Program for their support. RM is also acknowledging support of the BERC 2018-2021 program and Spanish Ministry of Science, Innovation and Universities through the Agencia Estatal de Investigacion (AEI) BCAM Severo Ochoa excellence accreditation SEV-2017-0718, and the Basque Government fund AI in BCAM EXP. 2019/00432.

References

1. Buskila, Y., Bellot-Saez, A., Morley, J.W.: Generating brain waves, the power of astrocytes. Front. Neurosci., 13, 1125 (2019).
2. Jain, K.K.: Neuroprotection in Alzheimer disease. In: The handbook of neuroprotection. 2nd edn. Humana Press, New York, pp. 465-585 (2019).
3. Ferrantelli, F., Chiozzini, C., Leone, P., Manfredi, F., Federico, M.: Engineered extracellular vesicles/exosomes as a new tool against neurodegenerative diseases. Pharmaceutics, 12(6), 529 (2020).
4. Pullan, J.E., Confeld, M.I., Osborn, J.K., Kim, J., Sarkar, K., Mallik, S.: Exosomes as drug carriers for cancer therapy. Mol. Pharmaceutics, 16(5), 1789-1798 (2019).
5. Luo, S., Du, L., Cui, Y.: Potential therapeutic applications and developments of exosomes in parkinson's disease. Mol. Pharmaceutics, 17(5), 1447-1457 (2020).
6. Kim, Y.S., Ahn, J.S., Kim, S., Kim, H.J., Kim, S.H., Kang, J.S.: The potential theragnostic (diagnostic+therapeutic) application of exosomes in diverse biomedical fields. Korean J. Physiol. Pharmacol, 22(2), 113–125 (2018).
7. Mizuma, A., Kim, J.Y., Kacimi, R., Stauderman, K., Dunn, M., Hebbar, S., Yenari, M.A.: Microglial calcium release-activated calcium channel inhibition improves outcome from experimental traumatic brain injury and microglia-induced neuronal death. Journal of Neurotrauma, 36(7), 996-1007 (2019).
8. Veletić, M., Barros, M.T., Arjmandi, H., Balasubramaniam, S., Balasingham, I.: Modeling of modulated exosome release from differentiated induced neural stem cells for targeted trug delivery. IEEE Trans. Nanobioscience, 19(3), 357-367 (2020).
9. Ganguly, M., Jenkins, M.W., Jansen, E.D., Chiel, H.J.: Thermal block of action potentials is primarily due to voltage-dependent potassium currents: a modeling study. J. Neural Eng., 16(3), 036020 (2019).
10. COMSOL Multiphysics® v. 5.5. www.comsol.com. COMSOL AB, Stockholm
11. Veletić, M., Barros, M.T., Balasingham, I., Balasubramaniam, S.: A molecular communication model of exosome-mediated brain drug delivery. In: NANOCOM '19, ACM, pp.1-7 (2019). doi:10.1145/3345312.3345478
12. Deng, Z., Wang, J., Xiao, Y., Li, F., Niu, L., Liu, X., Meng, L., Zheng, H: Ultrasound-mediated augmented exosome release from astrocytes alleviates amyloid-β-induced neurotoxicity. Theranostics, 11(9), 4351 (2021).